Introduction. This file includes pictures of sampling locations (Fig. S1), x-ray images of the coral samples (Fig. S2), photomicrographs of the coral samples (Figs. S3-S5), plots with Sr/Ca-SST anomalies and anomalies after detrending (Fig. S6), power spectrum analysis plots of non-detrended coral SST anomalies (Fig. S7) and SSA analysis plots (Figs. S8-S10) including text descriptions. Wavelet coherence plots (Fig. S11) and their text description, which support the power spectrum analysis plots in the main manuscript, are included in this file. Two additional tables giving the years of ENSO events used for the composite maps (Table S1) and the linear regression results between the coral SST records and the El Niño index Niño3.4 (Table S2) are also part of this supplementary material.

S1 Table with years of events that were used in the composite maps (Fig. 2)

Event years	
El Nino	La Nina
1982/83	1984/85
1986/87	1988/89
1987/88	1995/95
1991/92	1998/99
1994/95	1999/00
1997/98	2007/08
2002/03	2010/11
2009/10	2011/12
2015/16	

Table S1: El Niño and La Niña events years used for the composite maps. Between 1982 and 2016, 9 El Niño events occurred and 8 La Niña events occurred. Temperature anomalies from December to February were averaged for each event

S2 Pictures of coral sample sites

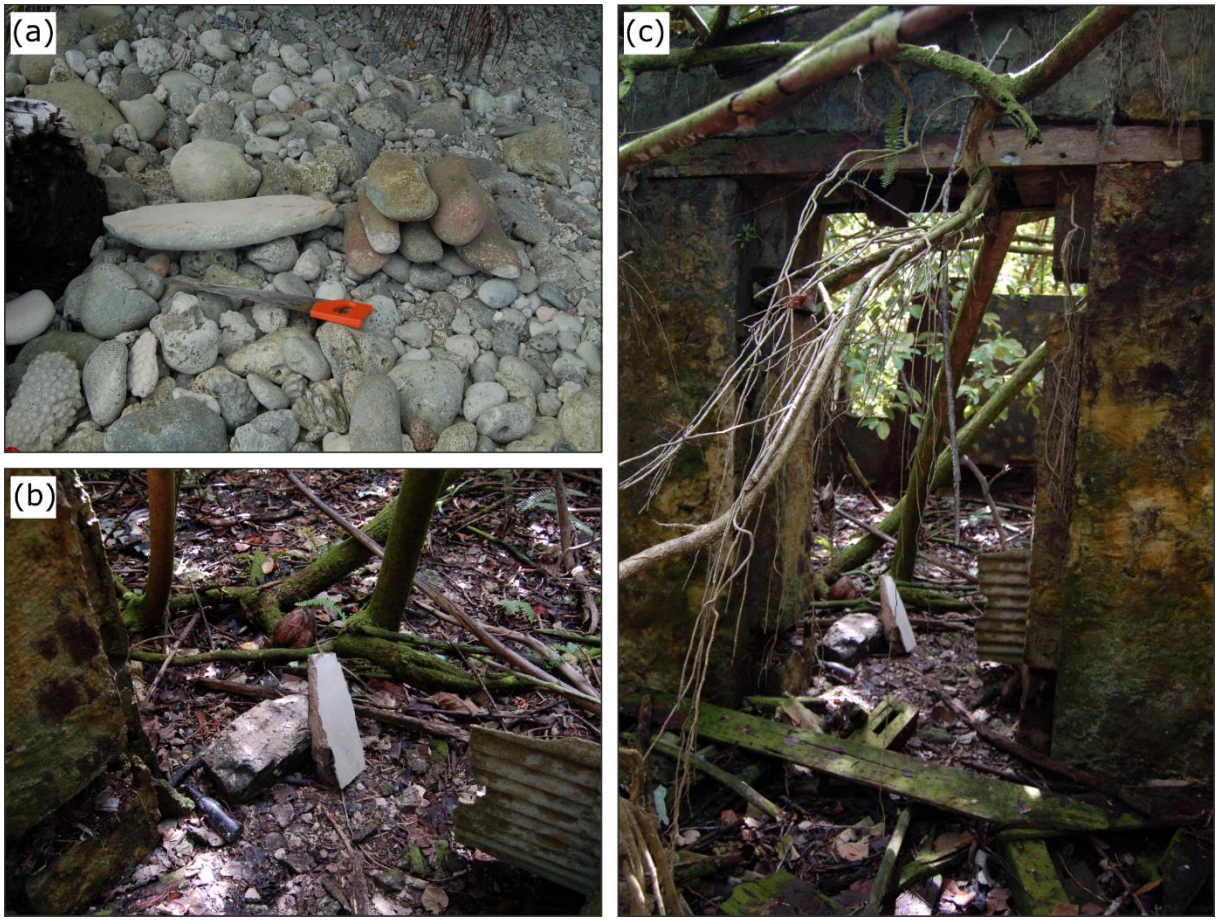

Figure S1: Pictures of coral sample sites. (a) Boulder beach at Eagle Island where the samples E5 (1675-1716) and E3 (1870-1909) were collected. (b) and (c) a derelict building at Boddam Island from which the sample B8 (1836-1867) was collected.

S3 X-ray images

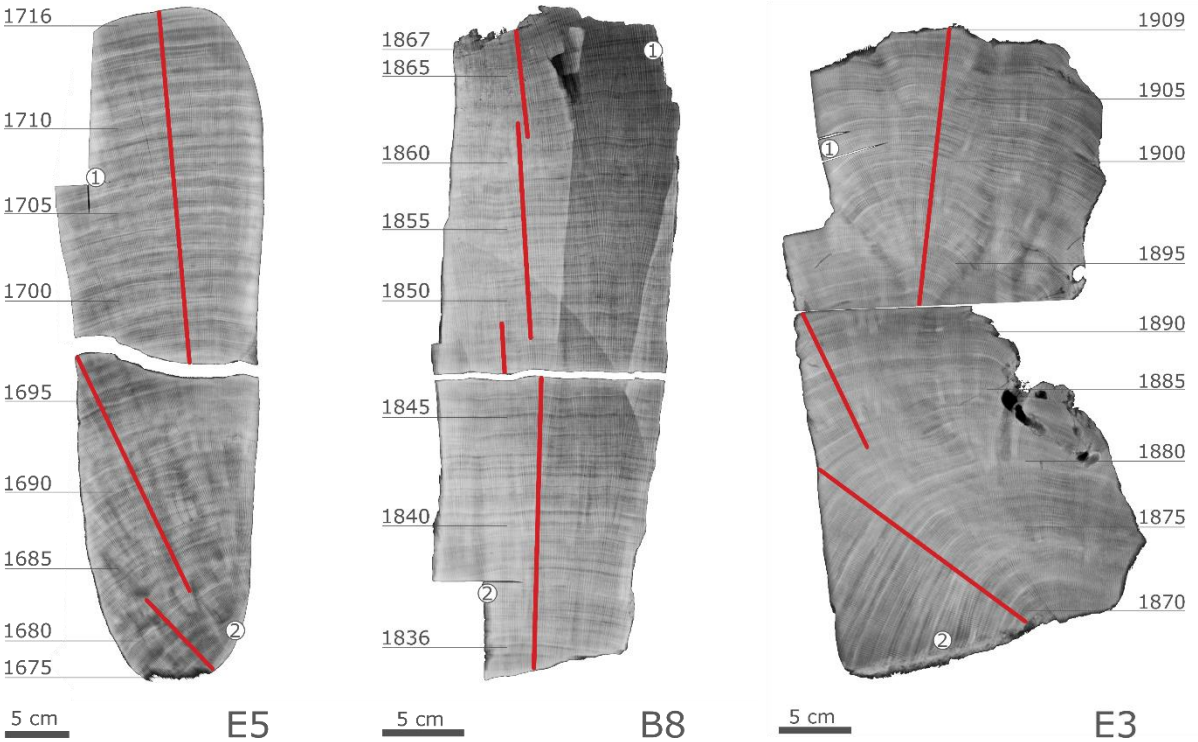

Figure S2: X-Ray images of coral samples analyzed in this study. Age models were interpreted using two U/Th measurements from each sample (sampling points for U/Th dating are indicated with circled numbers; for determined ages see Table 1). Red lines indicate subsampling paths.

S4 Thin section and SEM analysis images

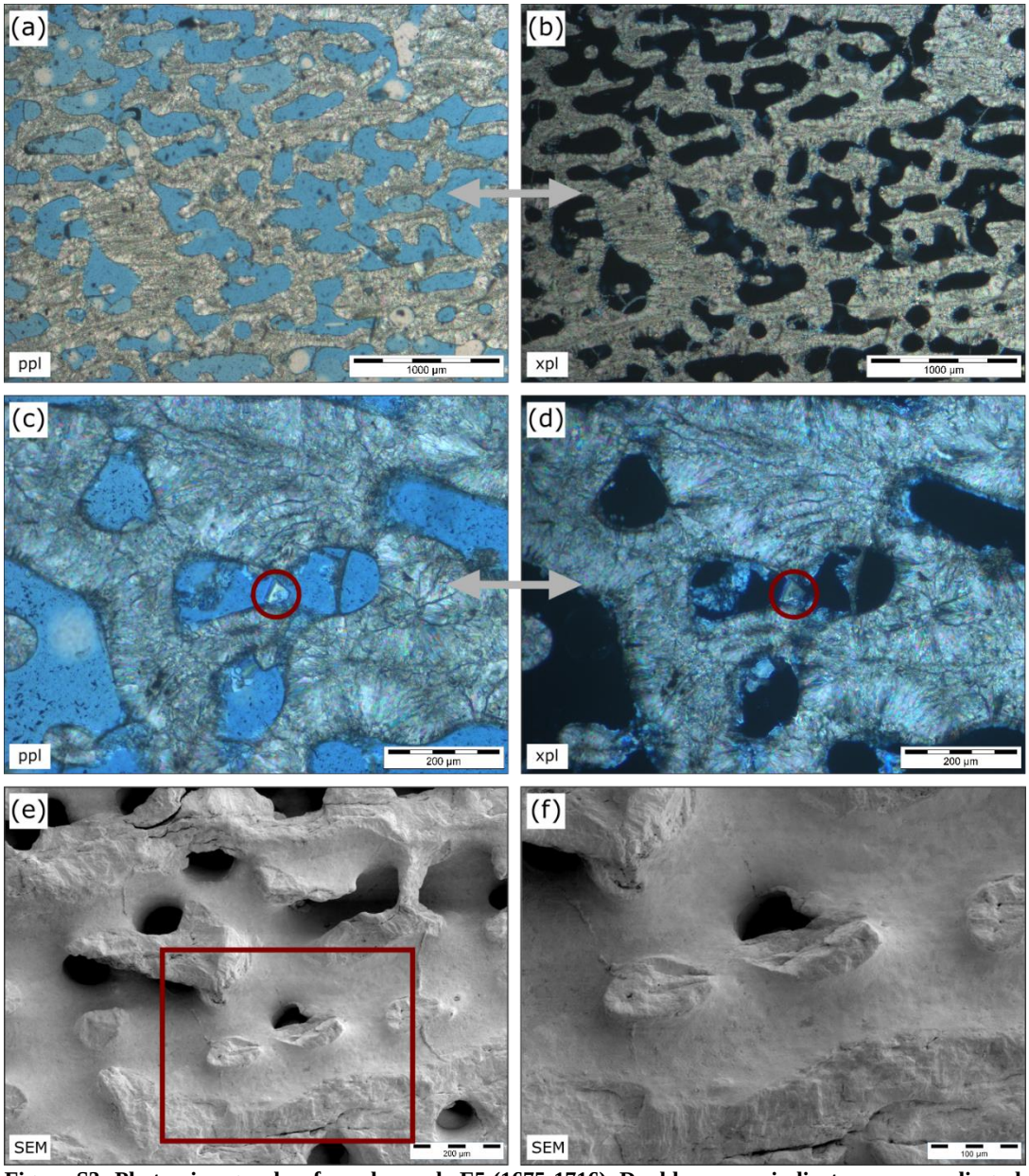

Figure S3: Photomicrographs of coral sample E5 (1675-1716). Double arrows indicate corresponding photomicrographs. (a) PPL and (b) XPL overview photomicrograph of the coral skeleton. (c) PPL and (d) XPL photomicrograph of higher resolution where minor amounts of secondary calcite cement is visible (red circle). (e) SEM overview and (f) SEM detail image of (e) where only trace amounts of sugary cements can be found.

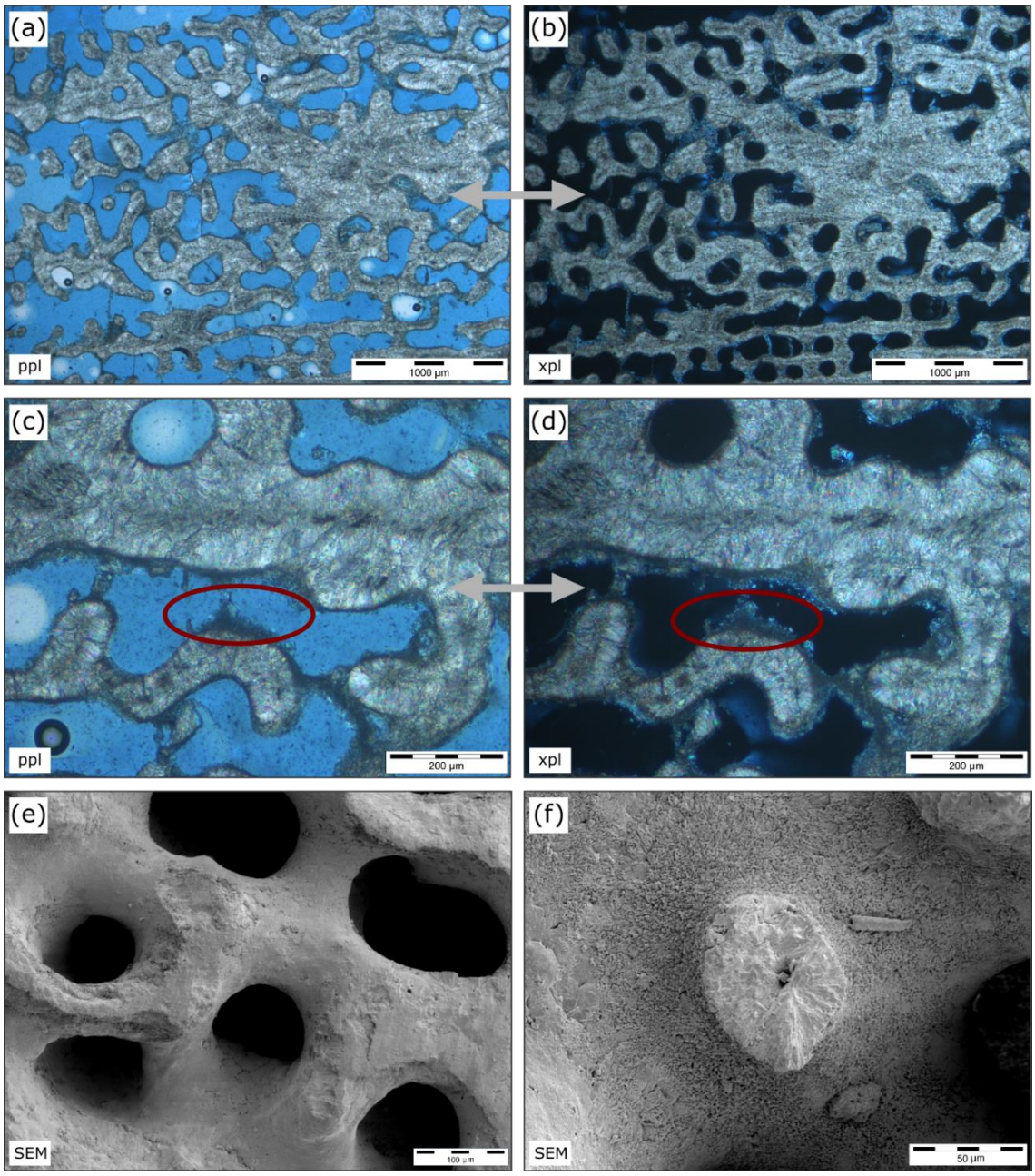

Figure S4: Photomicrographs of coral sample B8 (1836-1867). Double arrows indicate corresponding photomicrographs. (a) PPL and (b) XPL overview photomicrograph of the coral skeleton. (c) PPL and (d) XPL photomicrograph of higher resolution where small amounts of secondary aragonite cement is visible (red oval). (e) SEM overview image and (f) SEM detail image of B8 (1836-1867). Small amounts of sugary aragonitic cement can be seen.

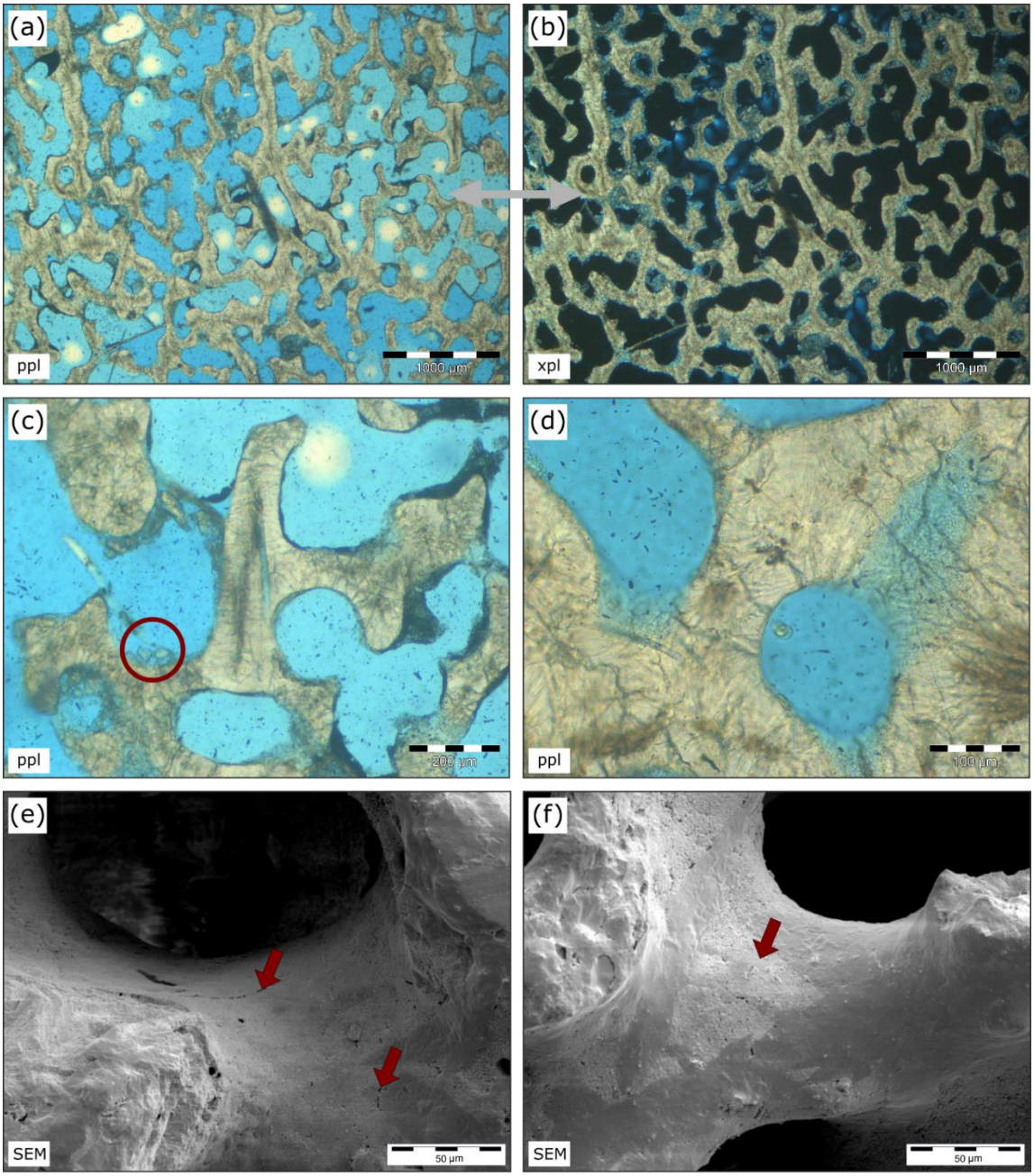

Figure S5: Photomicrographs of coral sample E3 (1870-1909). Double arrows indicate corresponding photomicrographs. (a) PPL and (b) XPL overview photomicrograph of the coral skeleton. (c) PPL photomicrograph of higher resolution where small fragments of aragonite are found (red circle). (d) PPL microphotograph of higher resolution with no signs of diagenesis. SEM images showing (e) microborings (red arrows) and (f) areas which appear brighter due to dissolution.

S4 Detrending of coral SST records

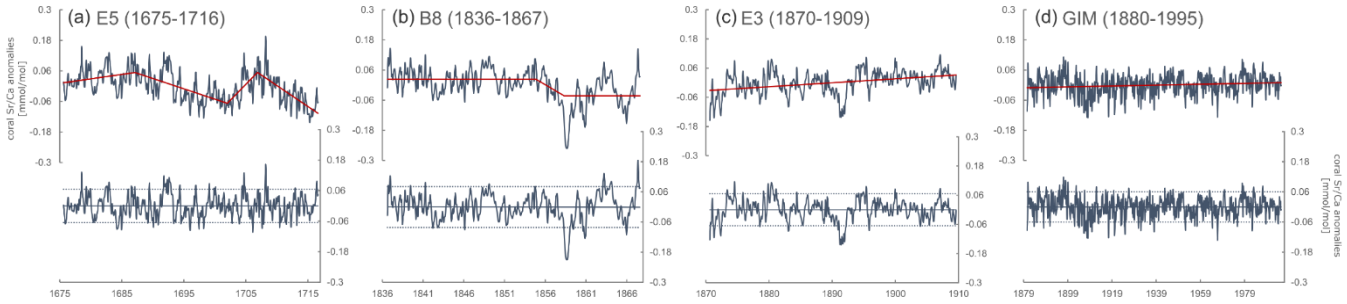

Figure S6: Sr/Ca-SST anomalies with calculated trend lines (red lines; upper plot) and anomalies after detrending (lower plot; with plotted 1.5x of the standard deviation as dashed lines) for the coral records (a) E5 (1675-1716), (b) B8 (1836-1867), (c) E3 (1870-1909) and (d) GIM (1880-1995).

S5 Seasonal cycles inferred from Singular Spectrum Analysis

Singular spectrum analysis (SSA) of the coral records with seasonal cycles reveal large interannual to decadal SST variabilities during both the 17-18th century and 19-20th century (not shown). The reconstructed components 2 and 3 (RC2, RC3) produced by SSA describe seasonal amplitudes for all samples and explain 28% (E5), 26% (B8), 32% (E3) of the coral Sr/Ca-SST variance. Decadal variabilities are larger during 17-18th century compared to 19-20th century. The first reconstructed component (RC1) for E5 with seasonal cycles explains 48% of the coral Sr/Ca-SST variance and describes a periodicity of around 18 years. Coral record covering the 19-20th century, lack a reconstructed component produced by SSA that describes decadal variability. Instead, RC1 explains 49% (B8) and 39% (E3) of the coral Sr/Ca-SST variance and describes a periodicity of around 7 years, which can be interpreted as ENSO periodicity.

The SSA results were validated by power spectrum analysis of bimonthly coral SST anomalies, which were not detrended (Fig. S7). To this analysis, the coral record GIM (Pfeiffer et al., 2017) was added. Power spectrum analysis of E5 (Fig. S7a) shows a low-frequency band corresponding to a periodicity of 18-19 years, identical to RC1 of the SSA. In addition, RC2 describing an ENSO periodicity of 4-5 years is confirmed by the second highest low-frequency band in power spectrum analysis of E5. The power spectrum analysis of the corals covering the 19-20th century (B8 and E3) confirms their SSA results, as well (Figs. S7b & c). It shows high power on the low-frequency (5-6 years for B8; 6-7 years for E3) band, which were also described by the first reconstructed components in SSA. Power spectrum analysis for GIM (Fig. S7d) reveals high power on the ENSO band (4-5 years and 8 years) and the highest power on the decadal frequency (26 years).

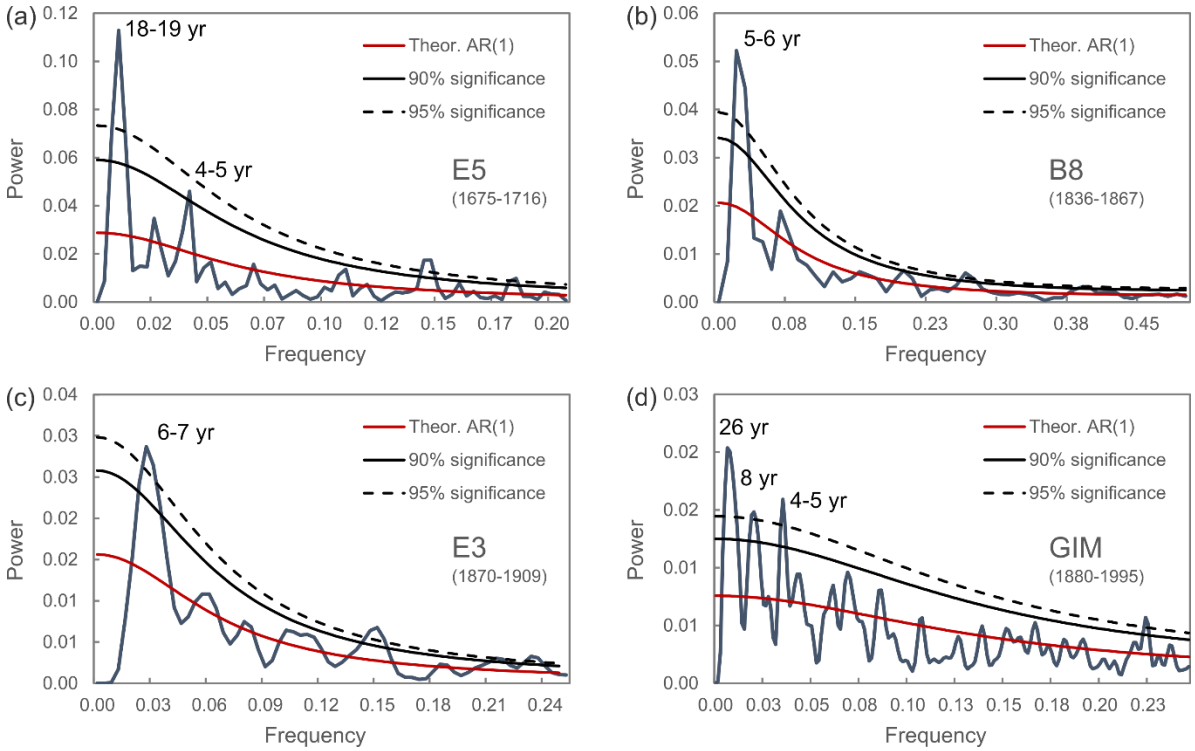

Figure S7: Power spectrum analysis of each Chagos coral bimonthly anomaly series.

S6 Interannual SST variability inferred from Singular Spectrum Analysis

The power spectrum analysis results were validated by singular spectrum analysis (SSA) with coral SST anomalies records, to reveal stronger patterns of variance when seasonal cycles were subtracted out (Figs. S8-S10). Still, but of minor percentage (9%), pattern of variance describing the seasonal cycles are found in the third reconstructed component for E5 (1675-1716) and B8 (1836-1867). During the 17-18th century, the coral record shows a periodicity of 18 years in RC1, which explains 47% of the coral Sr/Ca-SST variance (Fig. S8). The second reconstructed component (RC2; Fig. S8) of E5 (1675-1716) explains 14% of the coral Sr/Ca-SST variance and describes an ENSO periodicity of 4-5 years. During the 19-20th century, the pattern of variance describing the ENSO periodicity in the coral records are found in two to three reconstructed components: For B8 (1836-1867), RC2 and RC3 describe an ENSO periodicity of 5-8 years with, in total, 62% of the corals Sr/Ca-SST variability (Fig. S9). For E3 (1870-1909) it is even higher with RC1-3 explaining 65% of the coral Sr/Ca-SST variance. Those three components describe a characteristic ENSO periodicity of 3-8 years (Fig. S10).

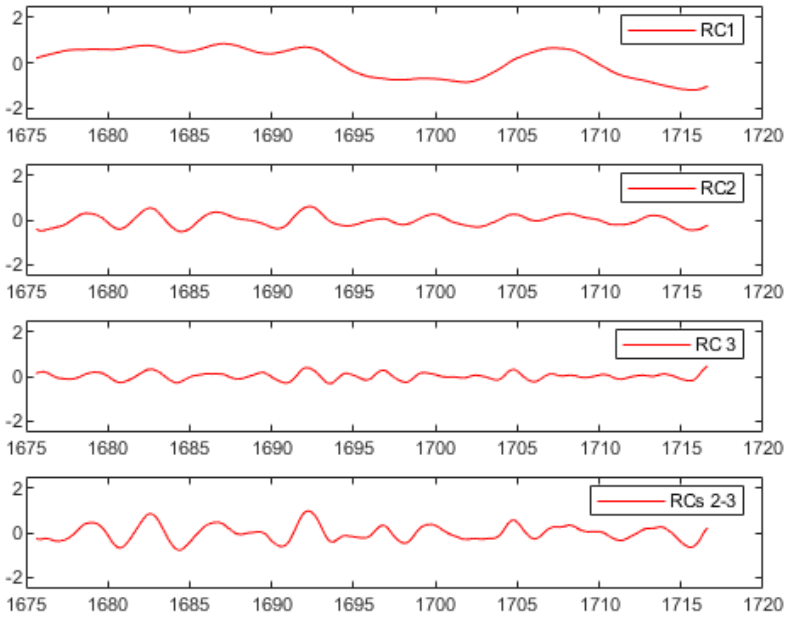

Figure S8: Reconstructed components from Singular Spectrum Analysis of E5 (1675-1716) Sr/Ca monthly anomalies. First reconstructed component (RC1) describes a periodicity of 18 years. RC2 and RC3 describe typical ENSO periodicities.

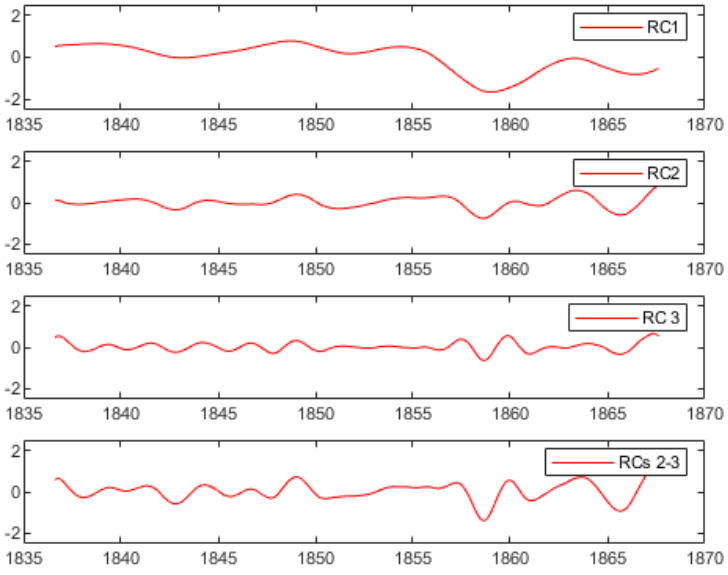

85

Figure S9: As Figure S8, but for coral Sr/Ca record of B8 (1836-1867).

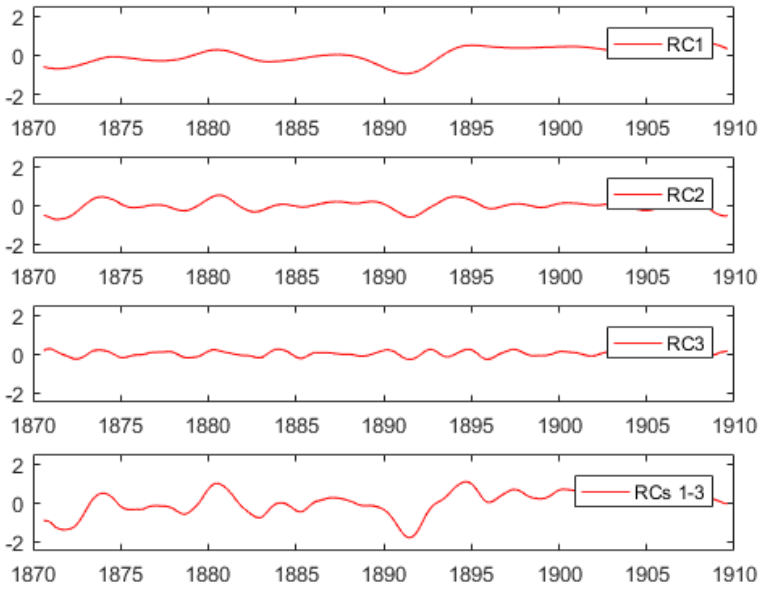

Figure S10: As Figures S8 and S9, but for coral Sr/Ca record of E3 (1870-1909) and ENSO periodicities are described by all shown reconstructed components RC1-3.

90

S7 Wavelet Coherence Analysis

To further investigate the relationship between the coral proxies and ENSO, Wavelet Coherence (WTC) was conducted on all coral records and the Nino3.4 index (Wilson et al., 2010).

Wavelet Coherence (WTC) plots were generated to find regions in time-frequency space where the *Nino3.4* index and the 95 Chagos coral SST records co-vary, even if they do not have high power in those regions (Fig. S11).

All WTC plots of the *Nino3.4* index and coral SST records reveal time-localized areas of strong coherence occurring in periods that correspond to the characteristic ENSO cycles of two to eight years. The WTC plots for the Nino3.4 index and the 19-20th century coral records show several regions where both time series co-vary. In contrast, the WTC plot of the *Niño3.4* index and the 17-18th century coral SST record shows only one region of co-variation at the beginning of the 18th century. The plots 100 show that there is an approximate delay of a 9 months to one year between the 17-18th century coral SST record and the Niño3.4 index (Fig. S11a), an approximate 1-3 year lag between B8 (1836-1867) and E3 (1870-1909), respectively, and the Nino3.4 index (Figs. S11b & c). However, the lags between the coral SST and the index time series are rather a result of the age model uncertainties than real time lags.

105

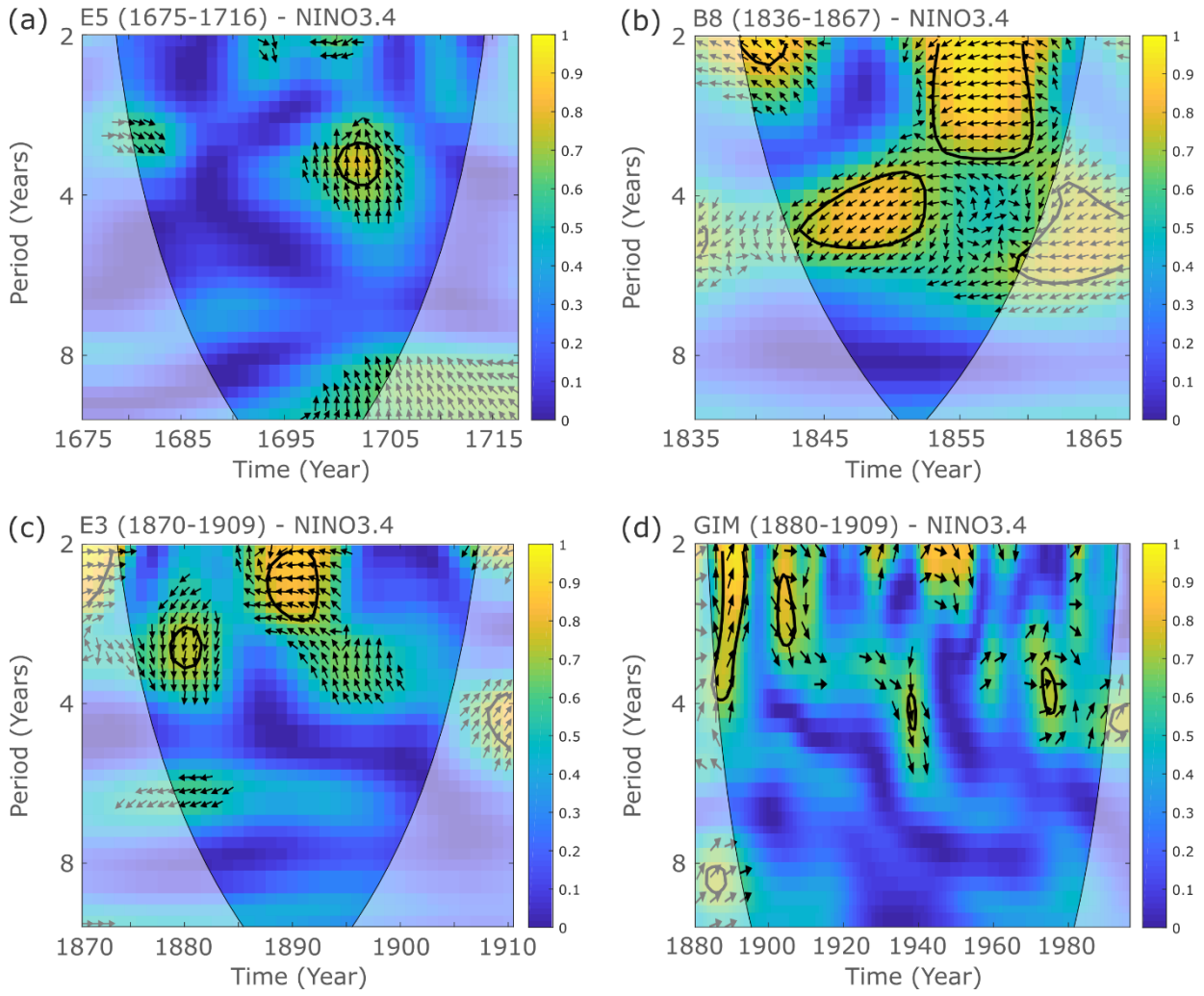

Figure S11: Wavelet coherence analysis plots for the Nino3.4 index and Chagos coral SST of (a) E5 (1675-1716), (b) B8 (1836-1867), (c) E3 (1870-1909) and (d) GIM (1980-1995).

S8 Linear regression

Ordinary least square (OLS) regression and *PearsonT3* calculation results reveal no significant linear relation between annual coral SST records and the El Niño index *Niño3.4* (Table S2).

Method	Coefficient	E5 (1675-1716)	B8 (1836-1867)	E3 (1870-1909)	GIM (1880-1995)
Excel OLS	R^2 (p-value)	4.09E-5 (0.9679)	0.0006 (0.8979)	0.0027 (0.7502)	0.0444 (0.0232)
PearsonT3	r [95% confidence interval]	-0.006 [-0.361; 0.350]	-0.024 [-0.739; 0.716]	0.052 [-0.418; 0.500]	0.211 [-0.005; 0.408]

Table S2: Correlation coefficients of given coral records with the Niño3.4 index.